Heliyon 10 (2024) e35423

Contents lists available at ScienceDirect

Heliyon

journal homepage: www.cell.com/heliyon

Research article

Jie-Du-Tong-Luo formula protects C2C12 myotubes against high glucose and palmitic acid injury by activating the PI3K/Akt/PPARγ pathway *in vitro*

Manying Wang [a], Xuenan Chen [a], Xiuci Yan [b], Changjiu Cai [c], Limei Ren [c], Shuai Zhang [d,**], Fangbing Liu [d,*]

[a] Research Center of Traditional Chinese Medicine, Affiliated Hospital to Changchun University of Chinese Medicine, Changchun, China
[b] Department of Clinical Laboratory, Affiliated Hospital to Changchun University of Chinese Medicine, Changchun, China
[c] Jilin Ginseng Academy, Changchun University of Chinese Medicine, Changchun, China
[d] Northeast Asian Institute of Traditional Chinese Medicine, Changchun University of Chinese Medicine, Changchun, China

ARTICLE INFO

Keywords:
Jie-Du-Tong-Luo formula
High glucose
Palmitic acid
C2C12 myotubes
PI3K/Akt/PPARγ

ABSTRACT

Introduction: In prior reports, Jie-Du-Tong-Luo (JDTL) was reported to help control insulin secretion and blood glucose in patients with diabetes, while also protecting liver and pancreatic islet cells against injury caused by exposure to high glucose (HG) levels. This study was thus developed to assess the effects of JDTL on HG and palmitic acid (PA)-induced muscle injury and to explore the mechanistic basis for these effects.
Methods: A model of muscle injury was established using mouse C2C12 myotubes treated with HG + PA. A proteomics approach was used to assess changes in protein levels following JDTL treatment, after which Western immunoblotting was employed to validate significantly affected pathways.
Results: JDTL was able to protect against HG + PA-induced muscle cell injury in this experimental system, altering lipid metabolism and inflammatory activity in these injured C2C12 myotubes. Western blotting suggested that JDTL is capable of activating PI3K/Akt/PPARγ signaling to control lipid metabolism without any corresponding impact on the inflammatory NF-κB pathway.
Conclusions: These data highlight the ability of JDTL to protect against HG + PA-induced injury to muscle cells, and suggest that the underlying basis for such efficacy is related to the PI3K/Akt/PPARγ pathway-mediated modulation of lipid metabolism.

1. Introduction

Diabetes is among the 10 most common chronic diseases in humans, with a prolonged course associated with a range of debilitating complications. The high levels of glucose and lipids in diabetic patients can cause damage to a range of tissues including the skeletal muscle, heart, eyes, kidneys, and blood vessels, resulting in widespread tissue dysfunction [1]. Skeletal muscle accounts for the largest proportion of human muscle tissue (40–50 %), and the existence of muscle lesions can contribute to movement disorders as well as an

* Corresponding author.
** Corresponding author.
E-mail addresses: zhangs530@nenu.edu.cn (S. Zhang), fangbing1993@outlook.com (F. Liu).

https://doi.org/10.1016/j.heliyon.2024.e35423
Received 19 September 2023; Received in revised form 20 July 2024; Accepted 29 July 2024
Available online 30 July 2024

elevated risk of stroke nad cardiovascular disease [2]. It is also one of the primary organs on which insulin acts, with muscles playing a central role in the regulation of appropriate glucose homeostasis [3]. There is thus a clear need to define appropriate interventions suitable for alleviating muscle injury caused by hyperglycemia nad hyperlipidemia in order to delay diabetes progression and to improve patient quality of life.

Traditional Chinese medicine (TCM) is a widely accepted form of alternative medical treatment throughout the world that offers key advantages attributable to its pleiotropic multi-target approach [4]. Jie-Du-Tong-Luo formula (JDTL) is composed of five herbal medicines including Coptis chinensis Franch (Huanglian), Radix Rhei Et Rhizome (Dahuang), *Astragalus propinquus* Schischkin (Huangqi), Salvia miltiorrhiza Bunge (Danshen), and Bupleuri Radix (Chaihu), at respective relative proportions (by weight) of 15:9:15:15:10. In clinical studies, JDTL intake in obese patients with diabetes was associated with lower levels of blood glucose and glycated hemoglobin together with the improvement of insulin secretion [5]. JDTL can also reportedly protect HepG2 and INS-1 cells [6], in addition to suppressing excess autophagic activity and ER stress in diabetic model rats to abrogate injury to pancreatic β-cells [7]. No prior studies, however, have examined the potential protective effects of JDTL on skeletal muscle.

In the present study, high glucose (HG) and palmitic acid (PA) were used to establish a model of muscle injury by treating murine C2C12 myoblasts. Proteomic assays were further used to screen for proteins and pathways impacted by HG and PA exposure and to identify pathways impacted by JDTL treatment for subsequent experimental verification.

2. Methods and materials

2.1. Materials

Mouse C2C12 myoblasts were obtained from the American Type Culture Collection (VA, USA). Fetal bovine serum (FBS) was from Clark Bioscience (VA, USA). Horse serum was from GIBCO (CA, USA). A BCA Protein Assay Kit was from Beyotime Biotechnology (Shanghai, China). Primary antibodies specific for phosphorylated PI3K (p-PI3K), PI3K, *p*-Akt, Akt, p-p65, p65, *p*-IκB, IκB, PPARγ, and GAPDH were from Cell Signaling Technology (MA, USA). Chemiluminescence reagents were from Santa Cruz Biotechnology (CA, USA).

2.2. JDTL extract preparation

JDTL extract formulations used for this study were prepared from five different medicinal herbs (Table 1), using a method published previously [6]. The utilized herbs were obtained from the Department of Pharmacy of the Affiliated Hospital of Changchun University of Chinese Medicine (Jilin, China). As per the standard procedures detailed in the 2015 edition of the Chinese Pharmacopoeia, 1 L of reverse osmosis water was used to suspend 15 g of Huanglian (Coptis chinensis Franch), 9 g of Dahuang (Radix Rhei Et Rhizome), 15 g of Huangqi (*Astragalus propinquus* Schischkin), 15 g of Danshen (Salvia miltiorrhiza Bunge), and 10 g of Chaihu (Bupleuri Radix), followed by simmering for 30 min at 100 °C until the volume was reduced to 300 mL. This process was repeated three times to produce a final aqueous extract that was filtered, centrifuged, and supernatants were freeze-dried under vacuum. The resultant powder was suspended at 100 mg/mL in dH_2O and filtered (0.2 μm), sterilized, and diluted for subsequent use.

2.3. Ultra-high-performance liquid chromatography (UHPLC) analyses of JDTL

To confirm the high quality of the utilized JDTL formulation, a UHPLC approach was used to assess its composition prior to use to conduct subsequent experiments. Briefly, 100 mg of sample was combined with 1 mL of 70 % methanol and ground (JXFSTPRP-48, 70Hz), and shaken for 3 min. After cooling, low-temperature ultrasonication (40 kHz) was performed, and samples were centrifuged (10 min, 12,000 rpm, 4 °C). Supernatants were filtered through 0.22 μm PTFE, and UHPLC analyses were conducted with a Thermo Vanquish UHPLC (Thermo Fisher, MA, USA) system. Chromatographic separation was performed with a Zorbax Eclipse C18 column (1.8 μm × 2.1 mm x 100 mm) (Agilent) at 30 °C with a gradient composed of 0.1 % formic acid in water (A) and acetonitrile (B) and a 0.3 mL/min flow rate. A Q-Exactive HF (Thermo Fisher) was used for tandem mass spectrometry analyses [8].

2.4. Cell culture and differentiation

C2C12 myoblasts were maintained in Dulbecco's Modified Eagle's Medium (DMEM) containing 25 mM glucose, 10 % foetal bovine serum, 100 units/mL penicillin and 100 μg/mL streptomycin and were incubated at 37 °C in humidified atmosphere with 5 % CO_2. At

Table 1
JDTL composition.

Chinese name	Latin name	Family	Weight (g)
Huanglian	Coptis chinensis Franch	Ranunculaceae	15
Dahuang	Radix et Rhizoma Rhei	Polygonaceae	9
Huangqi	Astragalus membranaceus	Leguminosae	15
Danshen	Salvia miltiorrhiza Bunge	Lamiaceae	15
Chaihu	Radix Bupleuri	Apiaceae	10

70%–80 % confluence, myoblasts were induced to differentiate into C2C12 myotubes by culturing them in DMEM with 25 mM glucose and 2 % horse serum for 5 d [9].

2.5. Treatment with HG, PA and/or JDTL

After 5 d of differentiation, C2C12 myotubes were subdivided into five groups: (1) the control group, in which cells were incubated for 24 h in medium; (2) the model group, in which cells were treated with 50 mM HG + 0.125 mM PA for 24 h; (3–5) the model group, in which cells were treated with 50 mM HG + 0.125 mM PA plus JDTL (50, 100, and 200 μg/mL) for 24 h. All groups were harvested for experiments.

2.6. MTT assay

C2C12 myoblasts were plated in 96-well plates (5×10^4 cells/mL), treated using HG (25 mM, 50 mM, 75 mM), PA (0.0625 mM, 0.125 mM, 0.25 mM, 0.5 mM, 1 mM), and/or JDTL (25 μg/mL, 50 μg/mL, 100 μg/mL, 200 μg/mL, 400 μg/mL), and MTT assays were conducted to assess viability [10]. Following a 4 h incubation with MTT reagent (0.5 mg/mL), 150 μL DMSO was added to solubilize formazan crystals, and absorbance at 490 nm was assessed. The percentage of cell viability relative to vehicle control treatment was computed.

2.7. Proteomic analyses

Cells were thawed from −80 °C and lysed via ultrasonication, followed by centrifugation (10 min, 12,000 g, 4 °C), and proteins in cell supernatants were assessed via BCA assay. Equal protein amounts were used for enzymatic hydrolysis, with peptide segments undergoing separation via UHPLC prior to introduction into an Orbitrap Exploris ™ 480 mass spectrometry system for analyses. Data were collected with a cycle time-based Data Dependent Scanning (DDA) program.

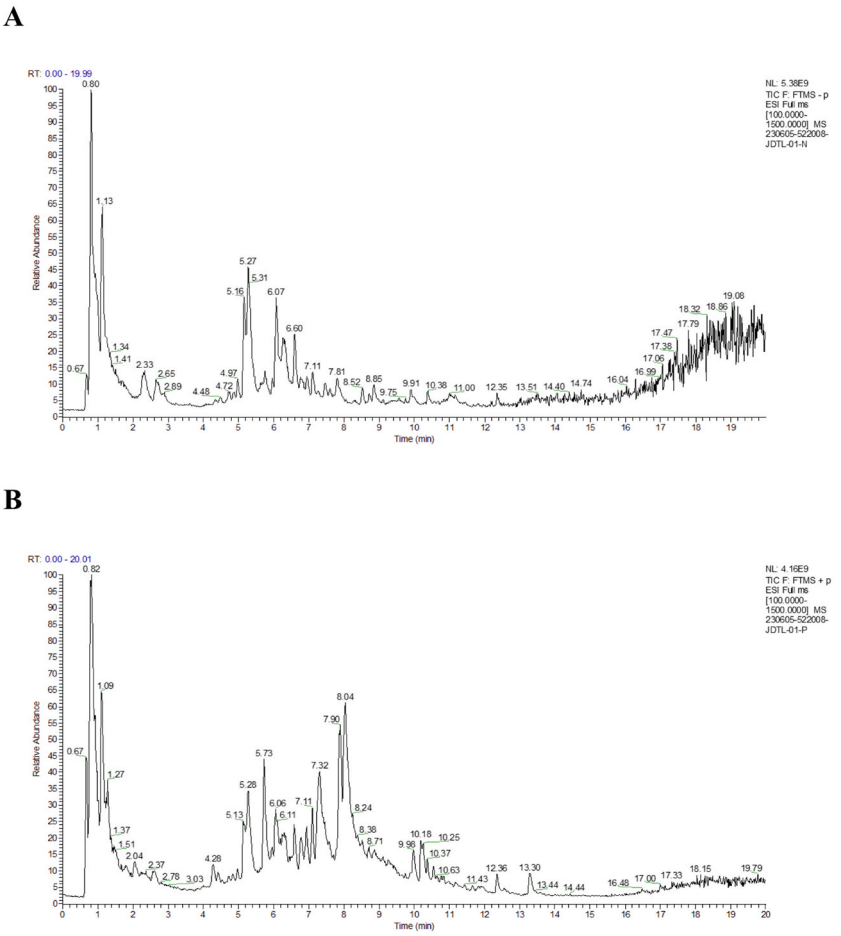

Fig. 1. Total ion chromatograms for JDTL generated using an UHPLC-Q-Exactive HF platform in (A) positive and (B) negative ion modes.

2.8. Western immunoblotting

After rinsing with PBS, cells were lysed for 30 min in RIPA buffer (Beyotime Biotechnology, Shanghai, China) before separation via 12 % SDS-PAGE and transfer onto PVDF membranes. These blots were blocked using 5 % bovine serum albumin, followed by overnight incubation with appropriate primary antibodies (1:1000) at 4 °C. After two washes, blots were incubated at room temperature for 1 h with secondary antibodies (1:5000). A chemiluminescent approach was used for protein detection as in prior reports (FluorChem HD2; ProteinSimple, CA, USA) [11].

2.9. Statistical analysis

Data are means ± SD from at least three independent experiments. Results were compared with one-way ANOVAs in GraphPad Prism 5.0 (GraphPad Software, CA, USA), with $p < 0.05$ serving as the threshold when defining significance.

Table 2
The chemical components of JDTL.

No.	RT (min)	Compounds	Molecular Formula	Expected Neutral Mass (Da)	Observed Neutral Mass (Da)	LC/MS (ESI ±) (*m*/*z*)	Mass Accuracy (ppm)	Adducts
1	0.82	Betaine	C5H11NO2	117.07898	117.07906	118.08636	0.7	$[M+H]^+$
2	2.795	Salvianic acid A	C9H10O5	198.05282	198.05217	198.04796	−3.32	$[M-H]^-$
3	4.69	Epicatechin	C15H14O6	290.07904	290.07865	291.05891	−1.34	$[M+H]^+$
4	4.97	Ferulic Acid	C10H10O4	194.05791	194.05772	195.06506	−0.98	$[M+H]^+$
5	5.248	Epicatechin	C15H14O6	290.07904	290.07898	291.08591	−0.21	$[M+H]^+$
6	5.302	Cryptochlorogenic acid	C16H18O9	354.09508	354.09495	353.08762	−0.36	$[M-H]^-$
7	5.61	Vanillic Acid	C8H8O4	168.04226	168.04213	169.04944	−0.78	$[M+H]^+$
8	5.987	Astringin	C20H22O9	406.12638	406.12633	405.11908	−0.12	$[M-H]^-$
9	6.445	Rutin	C27H30O16	610.15338	610.1536	611.15997	0.36	$[M+H]^+$
10	6.47	Isoquercitrin	C21H20O12	464.09548	464.09495	465.1022	−1.13	$[M+H]^+$
11	6.51	Calycosin-7-O-β-D-glucoside	C22H22O10	446.1213	446.12076	447.12814	−1.2	$[M+H]^+$
12	6.678	Isoquercitrin	C21H20O12	464.09548	464.09545	465.1022	−0.07	$[M+H]^+$
13	6.93	Oxyberberine	C20H17NO5	351.11067	351.11012	352.1174	−1.56	$[M+H]^+$
14	7.093	Lithospermic acid	C27H22O12	538.11113	538.11098	537.10376	−0.27	$[M-H]^-$
15	7.094	Quercitrin	C21H20O11	448.10056	448.09999	449.1073	−1.28	$[M+H]^+$
16	7.155	Emodin-3-methyl ether/ Physcion	C16H12O5	284.06847	284.06834	283.0611	−0.48	$[M-H]^-$
17	7.33	Jatrorrhizine	C20H19NO4	337.13141	337.13069	338.13794	−2.14	$[M+H]^+$
18	7.34	Epiberberine	C20H17NO4	335.11576	335.11534	336.12262	−1.25	$[M+H]^+$
19	7.458	Rosmarinic acid	C18H1O8	360.08452	360.08445	359.07724	−0.18	$[M-H]^-$
20	7.49	Emodin	C15H10O5	270.05282	270.05238	271.05969	−1.64	$[M+H]^+$
21	7.53	Salvianolic acid C	C26H20O10	492.10565	492.10525	493.11243	−0.8	$[M+H]^+$
22	7.78	Ononin	C22H22O9	430.12638	430.12601	431.1333	−0.87	$[M+H]^+$
23	7.811	Isoferulic acid	C10H10O4	194.05791	194.0571	193.04982	−4.18	$[M-H]^-$
24	7.82	Salvianolic acid A	C26H22O10	494.1213	494.12064	495.12778	−1.33	$[M+H]^+$
25	7.84	Salvianolic acid B	C36H30O16	718.15338	718.15252	719.15937	−1.2	$[M+H]^+$
26	7.85	Lithospermic acid	C27H22O12	538.11113	538.11065	539.11768	−0.88	$[M+H]^+$
27	8.28	Methylnissolin-3-O-glucoside	C23H26O10	462.1526	462.15201	463.15933	−1.26	$[M+H]^+$
28	8.415	Daidzein	C15H10O4	254.05791	254.05765	253.05037	−1.02	$[M-H]^-$
29	8.507	Isomucronulatol 7-O-glucoside	C23H28O10	464.16825	464.16842	463.16116	0.38	$[M-H]^-$
30	8.57	Methyl rosmarinate	C19H18O8	374.10017	374.10002	373.09277	−0.38	$[M-H]^-$
31	8.95	Chrysophanol 8-O-β-D-glucoside	C21H20O9	416.11073	416.11069	415.1034	−0.11	$[M-H]^-$
32	8.98	Calycosin	C16H12O5	284.06847	284.06791	285.07504	−1.98	$[M+H]^+$
33	10.00	Emodin-3-methyl ether/ Physcion	C16H12O5	284.06847	284.06799	285307502	−1.68	$[M+H]^+$
34	10.384	Saikosaponin D	C42H68O13	780.46599	780.46678	779.45959	1.01	$[M-H]^-$
35	10.39	Saikosaponin A	C42H68O13	780.46599	780.46513	781.47235	−1.1	$[M+H]^+$
36	10.47	Formononetin	C16H12O4	268.07356	268.07318	269.08051	−1.41	$[M+H]^+$
37	11.004	Rheic acid	C15H8O6	284.03209	284.03193	283.02469	−0.54	$[M-H]^-$
38	12.42	Dihydrotanshinone I	C18H14O3	278.09429	278.094	279.20129	−1.07	$[M+H]^+$
39	13.32	Cryptotanshinone	C19H2O3	296.14124	296.14085	297.14816	−1.33	$[M+H]^+$
40	14.48	Tanshinone IIA	C19H18O3	294.12559	294.12524	295.1326	−1.2	$[M+Na]^+$

3. Results

3.1. HPLC-MS/MS profiling of the composition of JDTL

A UHPLC-Q-Exactive HF system and the Compound Discoverer 3.3 application were initially employed to assess the chemical composition of JDTL. The total ion chromatograms and corresponding values pertaining to retention times, masses, and quasi-molecular and fragment ions are presented in Fig. 1A-B and Table 2.

3.2. JDTL enhances the viability of C2C12 myotubes injured by exposure to HG + PA

To select the most appropriate JDTL concentrations for experimental research, an MTT assay was used to evaluate the viability of JDTL-treated C2C12 myotubes. At doses below 400 μg/mL, JDTL treatment failed to impact viability at 24 h (Fig. 2A). Palmitic acid (PA), as the most abundant saturated fatty acid in the human body, has significant lipid toxicity and is suitable for establishing in vitro cell models. To establish a model of C2C12 myotube injury, these cells were treated with a range of HG and/or PA concentrations. HG alone did not impact myotube viability (Fig. 2B), and mannitol concentrations were also tested to examine the effects of osmotic pressure on these cells (Fig. 2C). Treatment with a 0.25 mM PA concentration for 24 h reduced C2C12 myotube viability to 78.88 ± 1.62 % (Fig. 2D), whereas co-incubation with 50 mM HG decreased viability to 72.31 ± 1.04 % (Fig. 2E). The effects of JDTL treatment (50–400 μg/mL) on this HG + PA-injured cell model was then assessed, revealing significant improvements in cellular viability (Fig. 2F). Overall, these data support the ability of JDTL to preserve the viability of C2C12 myotubes exposed to HG + PA-induced

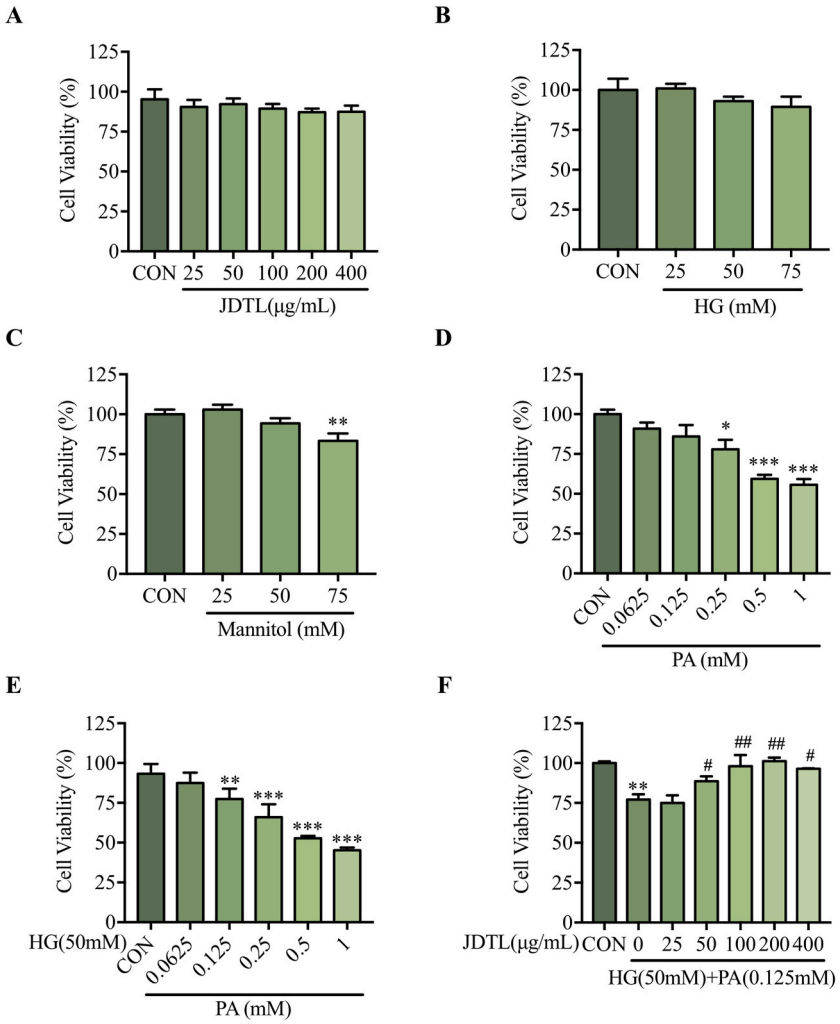

Fig. 2. The impact of JDTL on injury to C2C12 myotubes induced by exposure to HG and/or PA. (A–F) An MTT assay approach was used to assess the viability of C2C12 myotubes exposed to JDTL (A), HG (B), mannitol (C), PA (D), HG + PA (E), and HG + PA and JDTL. *$p < 0.05$, **$p < 0.01$, ***$p < 0.001$ vs. CON; #$p < 0.05$, ##$p < 0.01$ vs. HG + PA.

injury.

3.3. Differential protein screening

A principal component analysis was initially used to assess the repeatability of protein quantitation, revealing strong clustering and consistent repeatability in the three samples (Fig. 3A). Differentially abundant proteins were then analyzed with volcano plots (Fig. 3B) and heat maps (Fig. 3C). Relative to the control group, 133 downregulated and 193 upregulated proteins were identified, while relative to the model group, 30 downregulated and 15 upregulated proteins were identified following JDTL treatment (Fig. 3D).

3.4. Functional enrichment analyses of differentially abundant proteins

GO and KEGG enrichment analyses were next employed to explore the key pathways and processes associated with the myoprotective effects of JDTL in this assay system. JDTL treatment was found to have significant effects on a range of diabetes-related pathways related to lipopolysaccharide, oxidative stress, cytokine receptor binding, and cell proliferation, while also impacting various other biological process, cellular component, and molecular function terms (Fig. 4A–D). Pronounced enrichment related to

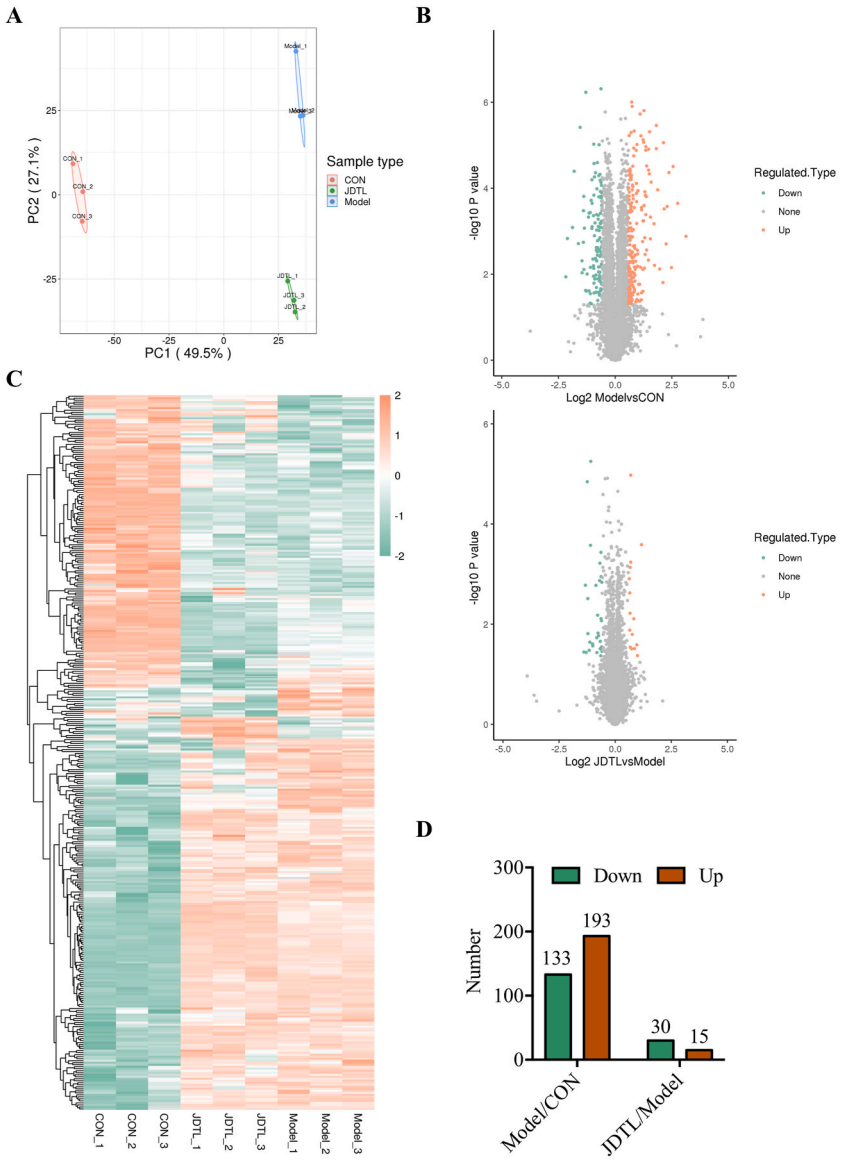

Fig. 3. Screening for differentially abundant proteins in JDTL-treated C2C12 myotubes injured with HG + PA. (A) Principal component analysis. (B) Volcano plot. (C) Heat map. (D) Column chart analysis.

inflammatory responses and lipid activity was noted, in line with prior evidence that these pathways are associated with the dysfunctional glycolipid metabolism and related pathological processes that underlie diabetes [12]. As such, the ability of JDTL to protect against diabetes-related damage may be related to the beneficial effects of its constituent components on these important biological functions.

3.5. JDTL activates PI3K/Akt/PPARγ pathway signaling in HG + PA-injured C2C12 myotubes

The above results suggested that JDTL may help protect against HG + PA-induced muscle injury through the modulation of inflammatory and lipid metabolism activity. As such, Western immunoblotting was next used to characterize the activity of the

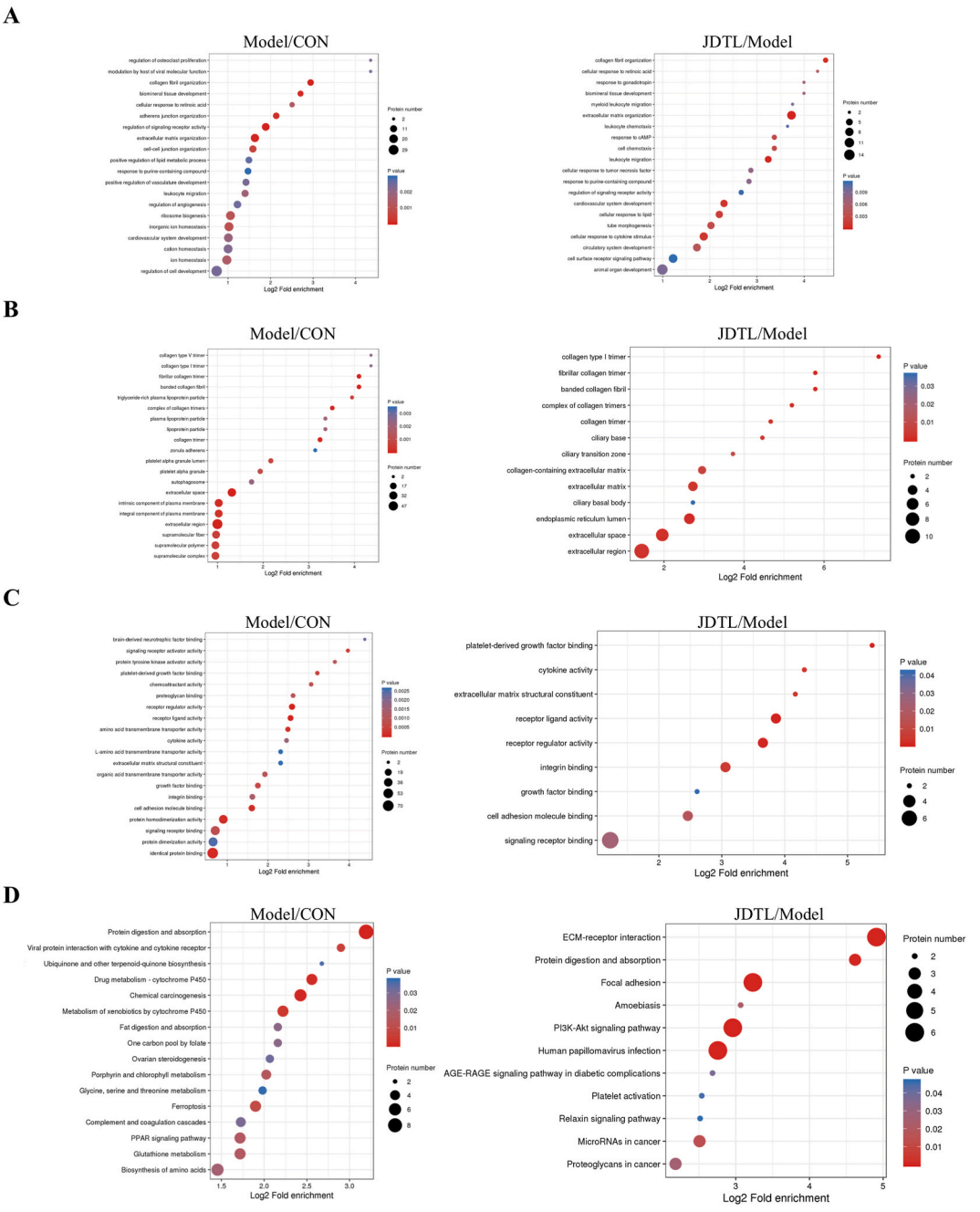

Fig. 4. Gene Ontology analyses of JDTL-treated HG + PA injured C2C12 myotubes. (A) Biological process terms. (B) Cellular component terms. (C) Molecular function terms. (D) KEGG pathway.

inflammation-related NF-κB pathway [13] and the lipid metabolism-related PPARγ pathway [14] and the upstream PI3K/Akt pathway. These analyses revealed reductions in PI3K and Akt phosphorylation in HG + PA-treated myotubes that were reversed by JDTL treatment (Fig. 5A and B). While HG + PA also increased p65 and IκB phosphorylation while reducing levels of PPARγ, JDTL only normalized PPARγ levels without significantly impacting p65 and IκB activity (Fig. 5A and C). These results suggest that JDTL is capable of improving the viability of C2C12 myotubes injured with HG + PA by enhancing the activity of the lipid metabolism-associated PI3K/Akt/PPARγ pathway.

4. Discussion

Diabetes is among the most devastating chronic diseases to affect humans owing to its prolonged course and high rates of complications [15]. Muscle is the most abundant tissue type in the body and the primary target organ of insulin, thus playing a central role in the incidence and progression of diabetes [16]. Clinical studies have demonstrated that skeletal muscle function and quality both decline in diabetic patients [17]. Some reports have suggested that muscle loss can be accelerated by insulin resistance, with consequent reductions in muscle mass further impairing normal glucose metabolism and thereby accelerating the development of insulin resistance. For these reasons, a growing number of researchers and clinicians have recognized the important role played by skeletal muscle in the incidence and progression of diabetes.

TCM is a practice that focuses on multi-target interventional strategies, achieving marked clinical success in the management of diabetes [18]. For example, the glucose intolerance and insulin sensitivity of mice fed a PA-containing diet were enhanced Ginseng-plus-Bai-Hu-Tang [19], while Yuye decoction can protect against dysfunctional pancreatic islet activity and may reverse or arrest the apoptotic death of islet β-cells [20]. Prior work from our team has demonstrated the protective effects of JDTL on HepG2 and INS-1 cells [6]. JDTL treatment of diabetic rats can also suppress excessive autophagy and ER stress to prevent damage to pancreatic β-cells [7]. Here, JDTL was further found to exert marked protective effects on C2C12 myotubes subjected to HG + PA injury.

A range of factors can account for diabetes-associated muscle damage driven by HG and PA, including oxidative stress [21], insulin resistance [22], and inflammatory activity [23]. Proteomics analyses revealed clear changes in the biological functions of HG + PA-treated C2C12 myotubes, while the beneficial effects of JDTL on these injured myotubes were primarily related to inflammatory and lipid-related processes. The PI3K/Akt pathway plays an important role in the regulation of both inflammation [24] and lipid metabolism [25]. Western immunoblotting subsequently confirmed the ability of JDTL to activate PI3K/Akt signaling and to regulate downstream PPAR**γ** pathway activity, thereby influencing lipid metabolic activity without any corresponding effects on the pro-inflammatory NFκB pathway or related mechanisms.

5. Conclusion

The present data revealed that JDTL is capable of regulating PI3K/Akt/PPARγ signaling to protect against HG + PA-induced injury

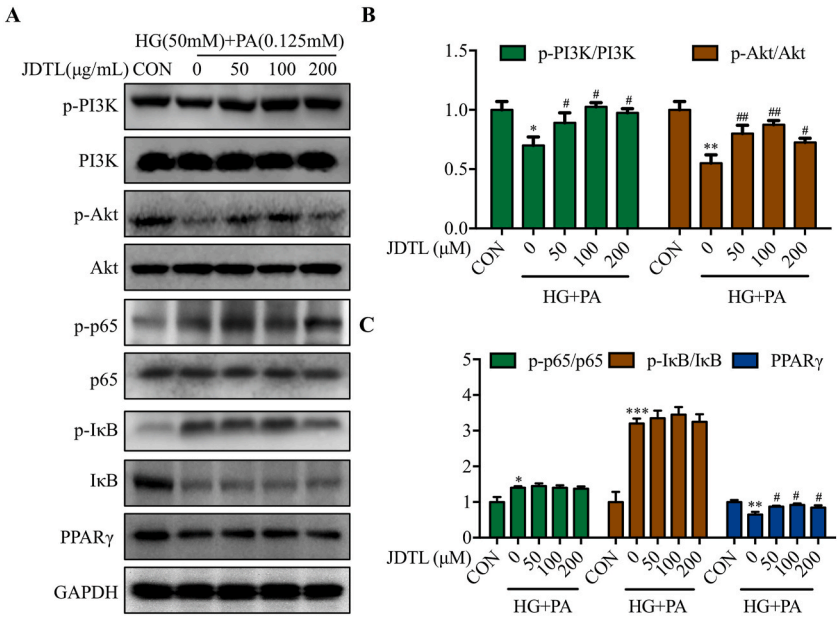

Fig. 5. JDTL activates PI3K/Akt/PPAR**γ** pathway signaling in C2C12 myotubes injured with HG + PA. (A–C) Following JDTL treatment for 24 h, p-PI3K/PI3K and *p*-Akt/Akt levels were assessed in HG + PA injured C2C12 myotubes via Western immunoblotting (A), with corresponding densitometric quantification of levels of p-PI3K/PI3K and *p*-Akt/Akt (B) and p-p65/p65, *p*-IκBα/IκBα, and PPAR**γ** (C) Data are means ± SD (n = 3). *p < 0.05, **p < 0.01, ***p < 0.001 vs. CON; #p < 0.05, ##p < 0.01 vs. HG + PA.

to muscle cells. This preparation thus holds great promise for use as an antidiabetic agent.

Data availability statement

The date was stored in iProX (https://www.iprox.cn/page/home.html). Username: Doris, Password: Doris.

CRediT authorship contribution statement

Manying Wang: Validation, Funding acquisition, Formal analysis. **Xuenan Chen:** Writing – original draft, Methodology, Formal analysis. **Xiuci Yan:** Investigation. **Changjiu Cai:** Software, Data curation. **Limei Ren:** Validation, Software. **Shuai Zhang:** Formal analysis, Conceptualization. **Fangbing Liu:** Visualization, Supervision.

Declaration of competing interest

The authors declare that they have no known competing financial interests or personal relationships that could have appeared to influence the work reported in this paper.

Acknowledgements

This work was supported by the National Natural Science Foundation of China (82204709, 82374380), the Science and Technology Development of Jilin Province (YDZJ202301ZYTS453, YDZJ202301ZYTS435). This work was supported by MJEditor (www.mjeditor.com) for its linguistic assistace during the preparation of this manuscript.

Abbreviations

JDTL	Jie-Du-Tong-Luo formula
HG	high glucose
PA	palmitic acid
UHPLC	Ultra-high-performance liquid chromatography

Appendix A. Supplementary data

Supplementary data to this article can be found online at https://doi.org/10.1016/j.heliyon.2024.e35423.

References

[1] C.R. Sen S, B. De, Complications of Diabetes Mellitus, Springer Singapore, 2016.
[2] L. Wang, T. Shan, Factors inducing transdifferentiation of myoblasts into adipocytes, J. Cell. Physiol. 236 (2021) 2276–2289.
[3] S. Maurotti, R. Pujia, A. Galluccio, S. Nucera, V. Musolino, R. Mare, M. Frosina, F.R. Noto, V. Mollace, S. Romeo, A. Pujia, T. Montalcini, Preventing muscle wasting: pro-insulin C-peptide prevents loss in muscle mass in streptozotocin-diabetic rats, J. Cachexia Sarcopenia Muscle 14 (2023) 1117–1129.
[4] J.O. Healthcare Engineering, Retracted: effects of insulin combined with traditional Chinese medicine assisted comprehensive nursing intervention on oxidative stress state, cell adhesion factor, and pregnancy outcome of patients with gestational diabetes mellitus, J. Healthc. Eng. 2023 (2023) 9864923.
[5] C. Piao, Q. Zhang, H. Fu, L. Wang, C. Tang, Effectiveness comparisons of catgut implantation at acupoint for obese type 2 diabetes: a protocol for systematic review and meta analysis, Medicine (Baltim.) 99 (2020) e21316.
[6] Q. Zhang, C. Piao, W. Jin, D. Jin, H. Wang, C. Tang, X. Zhao, N. Zhang, S. Gao, F. Lian, Decoding the chemical composition and pharmacological mechanisms of Jiedu Tongluo Tiaogan Formula using high-performance liquid chromatography coupled with network pharmacology-based investigation, Aging (Albany NY) 13 (2021) 24290–24312.
[7] J. Luo, W. Jin, M. Jin, W. Pan, S. Gao, X. Zhao, X. Lai, L. Sun, C. Piao, Jiedutongluotiaogan formula restores pancreatic function by suppressing excessive autophagy and endoplasmic reticulum stress, Pharm. Biol. 60 (2022) 1542–1555.
[8] X. Wang, X. Chang, X. Luo, M. Su, R. Xu, J. Chen, Y. Ding, Y. Shi, An integrated approach to characterize intestinal metabolites of four phenylethanoid glycosides and intestinal microbe-mediated antioxidant activity evaluation in vitro using UHPLC-Q-exactive high-resolution mass spectrometry and a 1,1-Diphenyl-2-picrylhydrazyl-Based assay, Front. Pharmacol. 10 (2019) 826.
[9] G. Xiang, K. Ying, P. Jiang, M. Jia, Y. Sun, S. Li, X. Wu, S. Hao, Growth differentiation factor 11 induces skeletal muscle atrophy via a STAT3-dependent mechanism in pulmonary arterial hypertension, Skelet Muscle 12 (2022) 10.
[10] M. Wang, X. Chen, W. Jin, X. Xu, X. Li, L. Sun, Ginsenoside Rb3 exerts protective properties against cigarette smoke extract-induced cell injury by inhibiting the p38 MAPK/NF-κB and TGF-β1/VEGF pathways in fibroblasts and epithelial cells, Biomed. Pharmacother. 108 (2018) 1751–1758.
[11] R. Jiang, M. Wang, L. Shi, J. Zhou, R. Ma, K. Feng, X. Chen, X. Xu, X. Li, T. Li, L. Sun, Panax ginseng total protein facilitates recovery from dexamethasone-induced muscle atrophy through the activation of glucose consumption in C2C12 myotubes, BioMed Res. Int. 2019 (2019) 3719643.
[12] Z. Cao, Z. Zeng, B. Wang, C. Liu, C. Liu, Z. Wang, S. Li, Identification of potential bioactive compounds and mechanisms of GegenQinlian decoction on improving insulin resistance in adipose, liver, and muscle tissue by integrating system pharmacology and bioinformatics analysis, J. Ethnopharmacol. 264 (2021) 113289.
[13] Q. Zhan, Y. Wu, L. Liu, Effects of notoginsenoside R1 on attenuating depressive behavior induced by chronic stress in rats through induction of PI3K/AKT/NF-κB pathway, Drug Dev. Res. 83 (2022) 97–104.
[14] H. Li, C. Yang, M. Lan, X. Liao, Z. Tang, Arctigenin promotes bone formation involving PI3K/Akt/PPARgamma signaling pathway, Chem. Biol. Drug Des. 95 (2020) 451–459.

[15] H. Sun, P. Saeedi, S. Karuranga, M. Pinkepank, K. Ogurtsova, B.B. Duncan, C. Stein, A. Basit, J.C.N. Chan, J.C. Mbanya, M.E. Pavkov, A. Ramachandaran, S. H. Wild, S. James, W.H. Herman, P. Zhang, C. Bommer, S. Kuo, E.J. Boyko, D.J. Magliano, IDF Diabetes Atlas: global, regional and country-level diabetes prevalence estimates for 2021 and projections for 2045, Diabetes Res. Clin. Pract. 183 (2022) 109119.
[16] S. Zhang, H. Yan, J. Ding, R. Wang, Y. Feng, X. Zhang, X. Kong, H. Gong, X. Lu, A. Ma, Y. Hua, H. Liu, J. Guo, H. Gao, Z. Zhou, R. Wang, P. Chen, T. Liu, X. Kong, Skeletal muscle-specific DJ-1 ablation-induced atrogenes expression and mitochondrial dysfunction contributing to muscular atrophy, J. Cachexia Sarcopenia Muscle 14 (2023) 2126–2142.
[17] D. Bassi-Dibai, A.D. Santos-de-Araujo, A.V. Dibai-Filho, L.F.S. de Azevedo, C.D.L. Goulart, G.C.P. Luz, P.R. Burke, A.S. Garcia-Araujo, A. Borghi-Silva, Rehabilitation of individuals with diabetes mellitus: focus on diabetic myopathy, Front. Endocrinol. 13 (2022) 869921.
[18] W. Zheng, G. Wang, Z. Zhang, Z. Wang, K. Ma, Research progress on classical traditional Chinese medicine formula Liuwei Dihuang pills in the treatment of type 2 diabetes, Biomed. Pharmacother. 121 (2020) 109564.
[19] H.F. Lu, Y.H. Lai, H.C. Huang, I.J. Lee, L.C. Lin, H.K. Liu, H.H. Tien, C. Huang, Ginseng-plus-Bai-Hu-Tang ameliorates diet-induced obesity, hepatic steatosis, and insulin resistance in mice, J. Ginseng Res. 44 (2020) 238–246.
[20] F. Guo, L. Yao, W. Zhang, P. Chen, R. Hao, X. Huang, J. Jiang, S. Wu, The therapeutic mechanism of Yuye decoction on type 2 diabetes mellitus based on network pharmacology and experimental verification, J. Ethnopharmacol. 308 (2023) 116222.
[21] Q. Ding, B. Sun, M. Wang, T. Li, H. Li, Q. Han, J. Liao, Z. Tang, N-acetylcysteine alleviates oxidative stress and apoptosis and prevents skeletal muscle atrophy in type 1 diabetes mellitus through the NRF2/HO-1 pathway, Life Sci. (2023) 121975.
[22] D.R. Pierce, M. McDonald, L. Merone, L. Becker, F. Thompson, C. Lewis, R.Y.M. Ryan, S.F. Hii, P.A. Zendejas-Heredia, R.J. Traub, M.A. Field, T. Rahman, J. Croese, A. Loukas, R. McDermott, P.R. Giacomin, Effect of experimental hookworm infection on insulin resistance in people at risk of type 2 diabetes, Nat. Commun. 14 (2023) 4503.
[23] R.C.R. Meex, E.E. Blaak, L.J.C. van Loon, Lipotoxicity plays a key role in the development of both insulin resistance and muscle atrophy in patients with type 2 diabetes, Obes. Rev. 20 (2019) 1205–1217.
[24] T. Roy, S.T. Boateng, M.B. Uddin, S. Banang-Mbeumi, R.K. Yadav, C.R. Bock, J.T. Folahan, X. Siwe-Noundou, A.L. Walker, J.A. King, C. Buerger, S. Huang, J. C. Chamcheu, The PI3K-Akt-mTOR and associated signaling pathways as molecular drivers of immune-mediated inflammatory skin diseases: update on therapeutic strategy using natural and synthetic compounds, Cells 12 (2023).
[25] L. Ren, X. Zhou, X. Huang, C. Wang, Y. Li, The IRS/PI3K/Akt signaling pathway mediates olanzapine-induced hepatic insulin resistance in male rats, Life Sci. 217 (2019) 229–236.